Magic Electron Counts for Networks of Condensed Octahedral Niobium Clusters in Oxoniobates

Grigori V. Vajenine and Arndt Simon*

Max-Planck-Institut für Festkörperforschung, Heisenbergstrasse 1, 70569 Stuttgart, Germany

Received December 22, 1998

Chemical bonding in networks of octahedral oxoniobate clusters condensed through vertex-sharing is analyzed at the extended Hückel level of theory. Crystal or molecular orbitals of the condensed cluster networks are derived from the Nb−Nb bonding molecular orbitals of the monomeric Nb_6O_{18} cluster. Extended networks are treated by considering crystal orbitals at special points of the corresponding Brillouin zones. We find that cluster electron counts corresponding to optimal bonding in these networks decrease from 14 for the Nb_6O_{18} cluster to 12 per Nb octahedron for a dimer, 11 for a linear chain of clusters, $10-10^1/_2$ for a square network of clusters, and $7^3/_4-8^1/_2$ for cubic NbO in which all cluster vertices are shared. These results are in good agreement with both the counts derived from the experimentally observed structures and a previously devised counting scheme. The loss of Nb−Nb bonding at the shared cluster vertices and the Nb−O−Nb π antibonding involving Nb atoms of neighboring octahedra are the reasons for the reduction of the magic cluster electron counts in the considered networks. It is proposed that similar counting schemes can be developed for other condensed cluster networks.

Introduction

Metal clusters in metal-rich compounds are favorite toys of experimental and theoretical chemists alike. Cluster condensation is one of the reasons for such interest. Condensed cluster systems, a link between molecule-like isolated clusters and three-dimensional metals, give rise to a variety of new structures[1] and provide theoreticians with tough but intriguing questions about bonding in such compounds.[2]

Reduced oxoniobates contain a remarkably complete set of condensed cluster compounds, which feature zero-, one-, two-, and three-dimensional substructures built from vertex-sharing niobium octahedra, as well as the monomeric Nb_6O_{18} clusters themselves. The review of oxoniobate compounds[3] also compares the electronic structure of Nb_6O_{18} to that of the condensed cluster networks. There a phenomenological electron counting scheme, which accurately describes all of the observed structures, is presented.

The goal of the present work is to develop further our understanding of chemical bonding in the networks of condensed oxoniobate clusters. By understanding we mean here being able to relate the molecular (or crystal) orbitals of condensed cluster networks to the well-known cluster orbitals of Nb_6O_{18} by carefully following through the effects of vertex-sharing. Such orbital construction also allows one to estimate the number of cluster electrons corresponding to optimal bonding in condensed cluster networks. These magic electron counts are compared to those derived from the previously devised counting scheme and to what is observed experimentally.

Structural Description of Condensed Oxoniobate Clusters

Figure 1 shows how two Nb_6O_{18} (or $Nb_6O^i_{12}O^a_6$, according to the standard notation[4]) clusters can be formally condensed by sharing a Nb vertex and four O^i atoms (with a loss of two O^a ligands) to form a $Nb_{11}O_{30}$ dimer. Such condensation can be continued by utilizing the remaining unshared Nb vertices to form a variety of condensed cluster networks. Note that the condensation takes place along three mutually orthogonal directions. Following a previously suggested notation,[3] we label the resulting networks as $[p \times q \times r]$, where p, q, and r are the numbers of niobium octahedra condensed along the three orthogonal directions.[5] Thus the monomeric Nb_6O_{18} cluster, found in more than 20 crystal structures,[3] acquires a $[1 \times 1 \times 1]$ label, $[1 \times 1 \times 2]$ stands for the dimer (as in $K_4Al_2Nb_{11}O_{21}$[6]), a linear one-dimensional infinite chain of condensed clusters is labeled $[1 \times 1 \times \infty]$ ($Ba_{1-x}Nb_5O_8$ with $x \approx 0.2$[7]), and a square two-dimensional network of clusters is refered to as $[1 \times \infty \times \infty]$ (as in MNb_4O_6 with M = K,[8] Ba[9−11] and in $M_2Nb_5O_9$ with

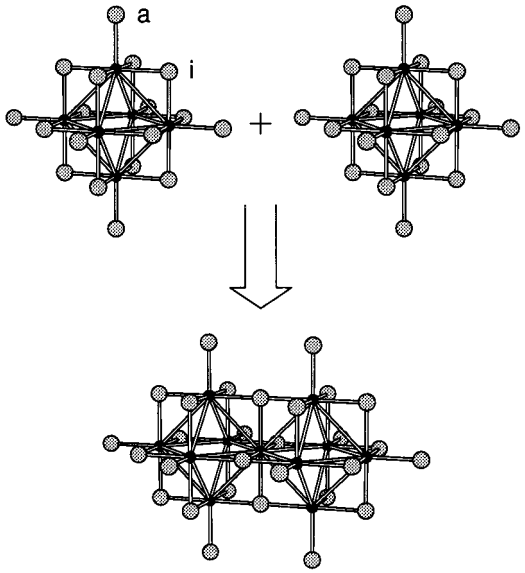

Figure 1. Formal condensation of two Nb_6O_{18} clusters to form a $Nb_{11}O_{30}$ dimer. The oxygen ligands are assigned labels according to the standard notation:[4] the *i* and *a* superscripts stand for inner (innen) and outer (aussen) coordination spheres, respectively.

(1) Simon, A. *J. Alloys Compd.* **1995**, *229*, 158−174.
(2) Hughbanks, T. *Prog. Solid State Chem.* **1989**, *19*, 329−372.
(3) Köhler, J.; Svensson, G.; Simon, A. *Angew. Chem., Int. Ed. Engl.* **1992**, *31*, 1437−1456.
(4) Schäfer, H.; Schnering, H. G. *Angew. Chem.* **1964**, *76*, 833−868.

10.1021/ic981460k CCC: $18.00
Published on Web 07/02/1999

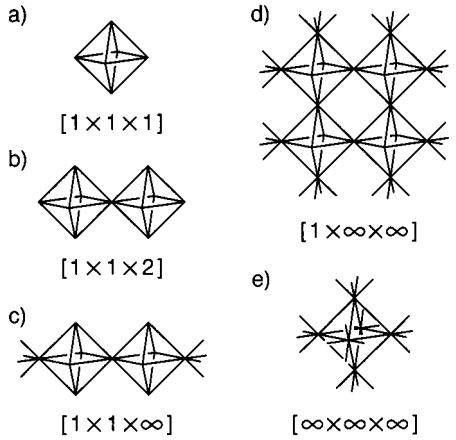

Figure 2. Cluster networks considered in this study (only the Nb backbones are shown): (a) a monomeric cluster, (b) a dimer, (c) a linear chain of clusters, (d) a square network of clusters, and (e) the cubic network of NbO.

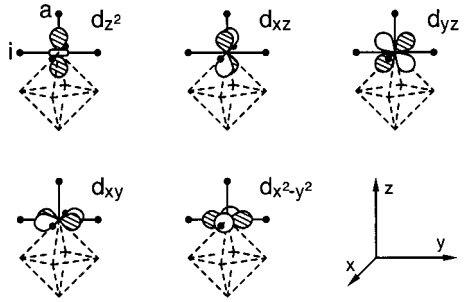

Figure 3. The notation used for the Nb 4d orbitals.

M = K,[12] Sr,[12−14] Ba,[9−12,15] and Eu[16]). The ultimate condensation utilizing all Nb vertices is achieved in the [∞ × ∞ × ∞] network of cubic NbO.[17] Figure 2 depicts some networks of condensed niobium clusters found in oxoniobates. The octahedral symmetry of the monomeric cluster is lost as vertex-sharing takes place. As a result, the Nb octahedra are no longer strictly regular in the networks of Figure 2b−d. Local octahedral symmetry is regained in NbO (Figure 2e).

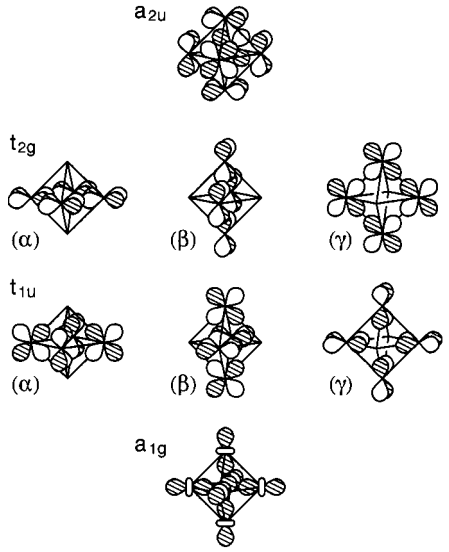

Figure 4. Drawings of the Nb−Nb bonding cluster orbitals of Nb_6O_{18}. Only major Nb 4d contributions are shown. For the t_{1u} and t_{2g} orbital sets only the 4d orbital contributions listed in the appropriate "×4" columns of Table 1 are given. These sets are also assigned the α, β, and γ labels for future reference.

There are several structural features that make condensation of Nb_6O_{18} clusters through vertex-sharing possible.[3] The first feature becomes apparent when examining the structure of the dimer (Figure 1): the shared niobium atom has to lie exactly in the plane of the four surrounding O^i ligands. For the vertex-sharing not to require a severe geometrical distortion, the niobium atoms in the Nb_6O_{18} cluster should not deviate much from the plane defined by the adjacent O^i ligands. In fact, this deviation is never greater than 0.05 Å.

The average Nb−Nb distance in octahedral clusters increases with the degree of condensation from 2.81 Å in the Nb_6O_{18} cluster to 2.98 Å in NbO. The overall increase of 0.17 Å is substantial; however, it constitutes only about 6% of the bond length. Therefore, the niobium octahedra can act as relatively rigid building blocks when forming condensed cluster networks.

These networks are not three-dimensional (with the exception of NbO) and have to be somehow assembled to form full crystal structures. $MNbO_3$ perovskite-type blocks with alkali, rare earth, or alkaline earth metals in the M site work well as spacers due to nearly perfect matches between the lattice constants of $MNbO_3$ and the size of the niobium octahedral clusters. Many oxoniobates are intergrowth phases of the $MNbO_3$-type (spacers) and NbO (clusters) structures.[15]

Computational Details

All calculations in this study were done using the extended Hückel method[18−20] with previously derived atomic parameters[21] for niobium[22,23] and oxygen.[23] The off-diagonal Hamiltonian

(5) Although not all theoretically conceivable networks of vertex-sharing niobium octahedra can be described using this convention, such notation is sufficient for the experimentally observed structures.
(6) Simon, A.; Köhler, J.; Tischtau, R.; Miller, G. *Angew. Chem., Int. Ed. Engl.* **1989**, *28*, 1662−1663.
(7) Zubkov, V. G.; Perelyaev, V. A.; Berger, I. F.; Kontsevaya, I. A.; Makarova, O. V.; Turzhevskii, S. A.; Gubanov, V. A.; Voronin, V. I.; Mirmil'shtein, A. V.; Kar'kin, A. E. *Sverkhprovodimost: Fiz., Khim., Tekn.* **1990**, *3*, 2121−2127.
(8) Svensson, G. *J. Solid State Chem.* **1991**, *90*, 249−262.
(9) Svensson, G.; Köhler, J.; Simon, A. *J. Alloys Compd.* **1991**, *176*, 123−132.
(10) Davydov, S. A.; Goshchitskii, B. N.; Karkin, A. E.; Mirmelstein, A. V.; Voronin, V. I.; Parkhomenko, V. D.; Zubkov, V. G.; Perelyaev, V. N.; Berger, I. F.; Kontzevaya, I. A. *Int. J. Mod. Phys. B* **1990**, *4*, 1531−1536.
(11) Zubkov, V. G.; Perelyaev, V. A.; Berger, I. F.; Voronin, V. I.; Kontsevaya, I. A.; Shveikin, G. P. *Dokl. Akad. Nauk SSSR* **1990**, *312*, 615−618.
(12) Michelson, C. E.; Rauch, P. E.; DiSalvo, F. J. *Mater. Res. Bull.* **1990**, *25*, 971−977.
(13) Svensson, G.; Köhler, J.; Simon, A. *Acta Chem. Scand.* **1992**, *46*, 244−248.
(14) Svensson, G. *Acta Chem. Scand.* **1990**, *44*, 222−227.
(15) Svensson, G. *Mater. Res. Bull.* **1988**, *23*, 437−446.
(16) Zubkov, V. G.; Perelyaev, V. A.; Kellerman, D. G.; Startseva, V. E.; Dyakina, V. P.; Kontsevaya, I. A.; Makarova, O. V.; Shveikin, G. P. *Dokl. Akad. Nauk SSSR* **1990**, *313*, 367−370.
(17) Bowman, A. L.; Wallace, T. C.; Yarnell, J. L.; Wenzel, R. G. *Acta Crystallogr.* **1966**, *21*, 843.
(18) Hoffmann, R.; Lipscomb, W. N. *J. Chem. Phys.* **1962**, *36*, 2179−2189.
(19) Hoffmann, R. *J. Chem. Phys.* **1963**, *39*, 1397−1412.
(20) Landrum, G. A. *Yet Another Extended Hückel Molecular Orbital Package (YAeHMOP)*, Cornell University, 1997. YAeHMOP is freely available on the World Wide Web at: http://overlap.chem.cornell.edu:8080/yaehmop.html.
(21) The following orbital energies, H_{ii}, and orbital exponents, ζ, were used: O 2s $H_{ii} = -32.3$ eV, $\zeta = 2.275$; O 2p $H_{ii} = -14.8$ eV, $\zeta = 2.275$; Nb 5s $H_{ii} = -10.1$ eV, $\zeta = 1.89$; Nb 5p $H_{ii} = -6.86$ eV, $\zeta = 1.85$. A double-ζ representation was employed for the Nb 4d orbitals: $H_{ii} = -12.1$ eV, $\zeta_1 = 4.08$, $c_1 = 0.6401$, $\zeta_2 = 1.64$, $c_2 = 0.5516$.

Table 1. Contributions (in %) of All Nb Orbitals (except $d_{x^2-y^2}$ which does not mix in) to the a_{1g}, t_{1u}, t_{2g}, and a_{2u} States of the Nb_6O_{18} Cluster. Contributions to the t Orbitals Are Split between Two Sets of Atoms, Using Representations as in Figures 4 and 5. The Corresponding Numbers for Nb_6O_{12} (with six O^a ligands removed) Are Given in Parentheses

	a_{1g}	t_{1u}		t_{2g}		a_{2u}
	×6	×2	×4	×2	×4	×6
d_{x^2}	39.84	14.04	0	0	0	0
	(71.64)	(30.66)	(0)	(0)	(0)	(0)
$d_{xz,yz}$	0	0	55.88	0	66.80	0
	(0)	(0)	(49.08)	(0)	(70.08)	(0)
d_{xy}	0	0	0	6.24	0	61.38
	(0)	(0)	(0)	(5.32)	(0)	(61.38)
all d	39.84	69.92		73.04		61.38
	(71.64)	(79.74)		(75.40)		(61.38)
s	9.60	1.14	0	0	0	0
	(18.48)	(3.50)	(0)	(0)	(0)	(0)
$p_{x,y}$	0	0	0.44	0	0.04	0
	(0)	(0)	(0.56)	(0)	(0.04)	(0)
p_z	21.18	5.72	0	0	0	0
	(3.00)	(1.14)	(0)	(0)	(0)	(0)
all Nb	70.62	77.22		73.08		61.38
	(93.12)	(89.94)		(75.44)		(61.38)

matrix elements were computed with the modified Wolfsberg−Helmholz formula.[24]

An idealized model geometry was assumed for niobium clusters and their condensates in all calculations. With the nearest neighbor Nb−Nb distances fixed at 2.85 Å and the Nb−O^i bond lengths set to $2.85/\sqrt{2} = 2.015$ Å, a square planar geometry was ensured for the NbO_4^i fragments. The Nb−O^a bond lengths were taken to be 2.25 Å (the average observed Nb−O^a distance[3]).

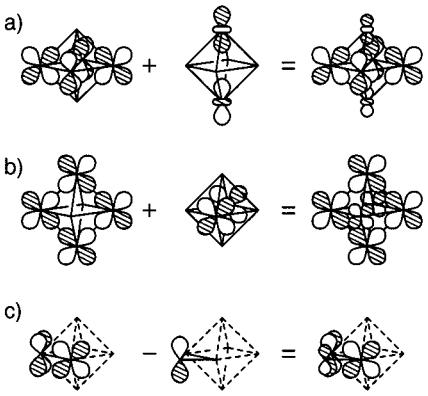

Figure 5. Minor Nb 4d contributions to the t_{1u} (a) and t_{2g} (b) orbital sets. These are listed in the appropriate "×2" columns of Table 1. Nb−O π antibonding in the a_{2u} orbital (c).

Bonding in an Isolated Nb_6O_{18} Cluster

We begin by considering the electronic structure of the Nb_6O_{18} cluster, the structural building block for the condensed cluster networks in oxoniobates. Bonding in Nb_6O_{18} has been described in detail elsewhere, for example, in the above-mentioned theoretical review;[2] we summarize these results below because they are the foundation of the following analysis.

The oxygen 2s and 2p levels in oxoniobates are completely filled, while the Nb 4d states are partially occupied, giving rise to Nb−Nb bonding. First, we take a look at the effect of the local Nb environment on the 4d orbitals (see also the related studies of bonding in NbO[23,25]).

The latter are depicted in Figure 3, with the O^i atoms lying along the *x* and *y* directions. The $d_{x^2-y^2}$ orbital in the $NbO_4^iO^a$

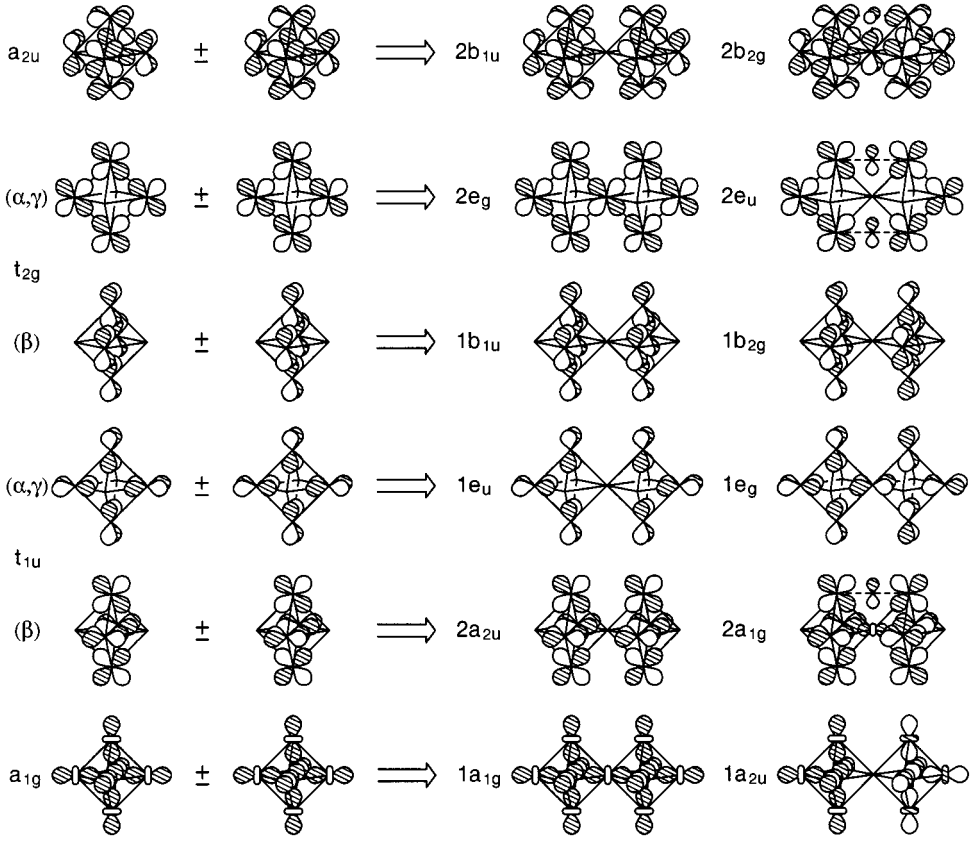

Figure 6. Construction of the dimer molecular orbitals using the a_{1g}, t_{1u}, t_{2g}, and a_{2u} icons of Figure 4. In this and in the following figures only major Nb 4d contributions are drawn out. For clarity not all symmetry equivalent O 2p contributions are shown.

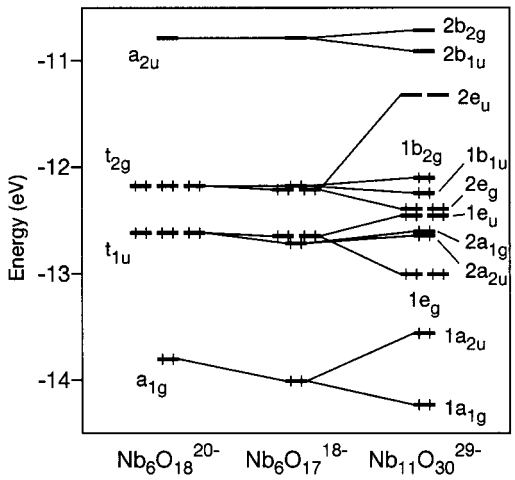

Figure 7. Computed correlation diagram relating molecular orbitals of the monomeric cluster to those of the dimer with Nb_6O_{17} as an intermediate step. Fourteen electrons are placed in the cluster orbitals of the monomer; orbitals of the dimer are filled with 24 electrons. The filled oxygen levels lie below −14.5 eV.

fragment (with O^a along the *z* axis) is oriented to interact with all four O^i ligands in a σ fashion. The d_{z^2} orbital interacts primarily with the O^a ligand, while the d_{xy}, d_{xz}, and d_{yz} wavefunctions are responsible for Nb−O π interactions. Such local coordinate system will be used to label the Nb 4d orbitals throughout our discussion.

The Nb−O^i σ antibonding pushes the $d_{x^2-y^2}$ orbital rather high in energy, leaving the other four Nb 4d orbitals for Nb−Nb bonding when the octahedral Nb_6O_{18} cluster is assembled. These four orbitals give rise to $6 \times 4 = 24$ cluster molecular orbitals. The lower eight of the latter (a_{1g}, t_{1u}, t_{2g}, and a_{2u} in octahedral symmetry) are Nb−Nb bonding; they are drawn out in Figure 4.

Table 1 summarizes Nb atomic contributions to these cluster orbitals. As expected, all of them have predominant Nb character, with the 4d wavefunctions contributing the most. The a_{1g} cluster orbital is formed mainly from d_{z^2}, with s and p_z also mixed in. Note that when the O^a ligands are pulled away to form the Nb_6O_{12} cluster (some or all six O^a ligands must be removed in order to allow for cluster condensation), the Nb−O antibonding in this orbital is reduced, as indicated by an increase of the overall Nb character due to increases in d_{z^2} and s contributions. The hypothetical Nb_6O_{18} to Nb_6O_{12} transformation also results in a drastic decrease of the p_z contribution, as it is no longer needed to hybridize this mainly d_{z^2} orbital away from the O^a ligands in order to reduce Nb−O^a antibonding. The t_{1u} states consist mainly of the Nb d_{xz} and d_{yz} wavefunctions, as depicted in Figure 4, with d_{z^2} mixed in as shown in Figure 5a. This mixing also depends on whether the O^a ligands are included in calculations. The d_{xz} and d_{yz} wavefunctions give rise to the t_{2g} orbital set as well, the other contribution coming from d_{xy} (Figure 5b). The Nb 5s and 5p wavefunctions play only a minor role in the t_{1u} and t_{2g} orbitals.

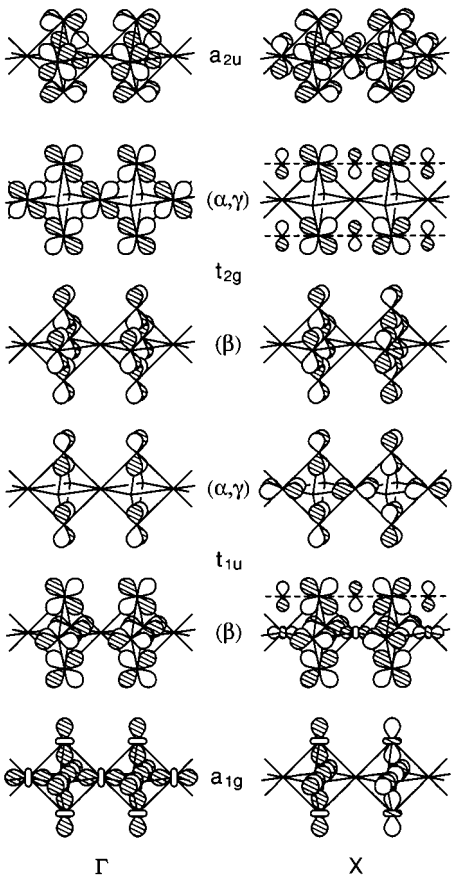

Figure 8. Crystal orbitals of a linear chain of vertex-sharing clusters at the Γ and X points of the Brillouin zone.

The a_{1g}, t_{1u}, and t_{2g} cluster orbitals are also weakly Nb−O antibonding, but the Nb−Nb bonding dominates. Of all Nb wavefunctions only d_{xy} contributes to the a_{2u} cluster orbital, in which for every Nb−Nb π bonding contact there are two Nb−O π antibonding ones (Figure 5c). The Nb−O antibonding wins, disfavoring occupation of this orbital.

Thus the 14 electron count is the magic one for the Nb_6O_{18} cluster. The 16 cluster electron count is observed in corresponding halides, where weaker metal−ligand π antibonding interactions do not prevent the a_{2u} orbital from becoming occupied.

We stress one important feature of this well-known result; that is how it can be presented. An octahedral cluster has 6 vertices, 12 edges (bonds), and 8 triangular faces. Thus the 14 (16) magic cluster electron count can be also stated as the $2^1/_3\bar{e}$ ($2^2/_3\bar{e}$) per atom, $1^1/_6\bar{e}$ ($1^2/_6\bar{e}$) per bond, or $1^3/_4\bar{e}$ ($2\bar{e}$) per triangular face count. Although these seemingly simpler counting approaches can be used as starting points in other descriptions of bonding in condensed cluster compounds (as, for example, in the above-mentioned review of oxoniobate chemistry[3]), the "per octahedron" count, derived from the molecular orbital picture, brings us much closer to understanding bonding in Nb_6O_{18}.[26]

(22) Summerville, R. H.; Hoffmann, R. *J. Am. Chem. Soc.* **1976**, *98*, 7240−7254.
(23) Burdett, J. K.; Hughbanks, T. *J. Am. Chem. Soc.* **1984**, *106*, 3101−3113.
(24) Ammeter, J. H.; Bürgi, H.−B.; Thibeault, J. C.; Hoffmann, R. *J. Am. Chem. Soc.* **1978**, *100*, 3686−3692.
(25) Andersen, O. K.; Satpathy, S. in Dominguez, A.; Castaing, J.; Marquez, R., Eds. *Basic Properties of Binary Oxides;* Publ. Univ. Sevilla: 1983; pp 21−42.

(26) The "per triangular face" counting approach is actually successful for the halide clusters with 16 electrons: two electrons per triangular face can be attributed to a three-center two-electron bond, with eight such bonds holding the metal cluster together. However, such approach is not general, as it breaks down when applied to oxide clusters with 14 electrons due to an overcompensation of M−M bonding by M−O antibonding interactions. The "per bond" count works in some M_6L_8 clusters, where the ligands cap triangular faces of the metal octahedron: the often-observed 24 cluster electron count can be interpreted as 12 "standard" two-center two-electron M−M bonds.

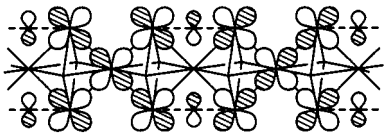

Figure 9. One possible representation of the t_{2g} (α,γ) band at the $k = \pi/2a$ point.

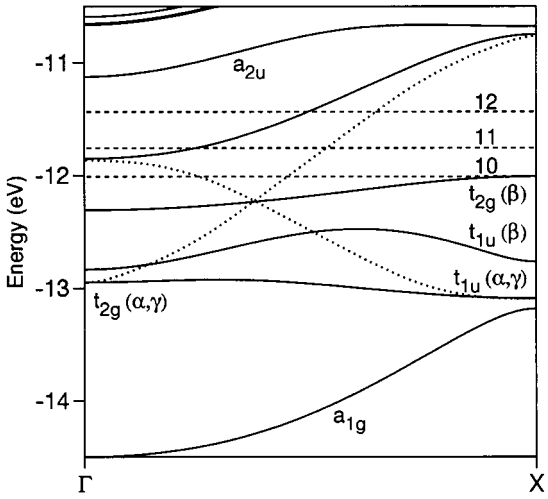

Figure 10. Computed band structure of the linear chain of condensed clusters. The character of bands does not change from Γ to X except for the t_{1u} (α,γ) and t_{2g} (α,γ) bands, which undergo an avoided crossing (dotted lines). Dashed lines indicate the positions of the Fermi level for 10, 11, and 12 electrons per Nb octahedron.

Cluster Dimerization

The dimeric $Nb_{11}O_{30}$ cluster, or the [1 × 1 × 2] cluster block, is the first step in the oxoniobate cluster condensation. The electronic structure of the dimer has already been calculated and discussed.[6]

We concentrate on establishing a link between the orbitals of condensed cluster networks and the molecular orbitals of Nb_6O_{18}. Therefore, we use the simplified graphical representations of the a_{1g}, t_{1u}, t_{2g}, and a_{2u} orbitals from Figure 4, in the following called "icons", in an attempt to construct the cluster molecular orbitals of the dimer. This construction is depicted in Figure 6.

Each of the eight Nb−Nb bonding orbitals of Nb_6O_{18} leads to two dimer orbitals (a plus and a minus combination), a total of 16 states. Next we go through the details of this construction.

The d_{z^2} wavefunction of the shared niobium atom is allowed to contribute to the $1a_{1g}$ dimer orbital, but not to $1a_{2u}$. Thus the former orbital looks essentially like its a_{1g} building blocks, while the lost Nb d_{z^2} − Nb d_{z^2} bonding in the latter is only partially compensated by a weak mixing of the Nb p_z wavefunction at the common vertex (this mixing is not shown in Figure 6).

The $2a_{2u}$ and $2a_{1g}$ dimer orbitals are assembled from the β component of the t_{1u} set. The central niobium atom in $2a_{2u}$ is allowed to contribute only its p_z wavefunction (not shown), while the shared O^i ligands contribute nothing at all. The Nb−O^i−Nb π antibonding interactions between the Nb octahedra are allowed by symmetry in $2a_{1g}$, but they are balanced by the Nb−Nb bonding as the d_{z^2} orbital of the central niobium also mixes in.

The $1e_u$ and $1e_g$ dimer orbitals, arising from the t_{1u} (α,γ) building blocks, also differ significantly at the shared vertex: the $1e_g$ orbitals remain very similar to the parent building blocks, while a weak $p_{x,y}$ mixing at the shared vertex (not shown) in $1e_u$ again only partially compensates for the loss of Nb−Nb bonding. We also note that a d_{z^2} mixing, similar to that depicted in Figure 5a, takes place in both $1e_g$ and $1e_u$ orbitals.

Most of the Nb−Nb bonding is retained in the $1b_{1u}$ and $1b_{2g}$ dimer orbitals. The d_{xy} wavefunction of the shared niobium atom is allowed to contribute in a bonding fashion to $1b_{1u}$ (similar to mixing shown in Figure 5b; not depicted in Figure 6), but not to $1b_{2g}$.

The $2e_g$ orbitals of the dimer are similar to the parent t_{2g} (α,γ) orbitals of the monomeric cluster; strong Nb−Nb bonding to the shared vertex is also preserved. Notably, the Nb−O^i−Nb π antibonding involving Nb atoms of different octahedra is not allowed. The $2e_u$ orbital, on the other hand, features such π antibonding and lacks the contribution of the central niobium atom. The Nb $p_{x,y}$ orbitals there are allowed by symmetry to take place of the inactive $d_{xz,yz}$, but do not do so due to the antibonding contacts with the 2p wavefunctions of the shared O^i ligands.

Lastly, the $2b_{1u}$ and $2b_{2g}$ orbitals of the dimer both feature substantial Nb−O π antibonding (two Nb−O π antibonding interactions for every Nb−Nb π bonding one), much like the parent a_{2u} orbital.

The Nb−O π antibonding across the linear Nb−O^i−Nb bridges has been given special consideration for the following reason. The Nb−O^i−Nb π antibonding in the Nb_6O_{18} cluster is rather strong when one of the three O^i 2p orbitals, the one perpendicular to the plane of the Nb−O^i−Nb triangle, participates, as in the a_{2u} orbital (Figure 5c). We recall that such antibonding leads to a significant destabilization of the a_{2u} orbital in the monomeric cluster. The two remaining O^i 2p orbitals can interact with wavefunctions of only one of the two bridged niobium atoms at a time, resulting in weaker antibonding.[27] The linear Nb−O^i−Nb geometry, a consequence of cluster condensation through vertex-sharing, allows two of the three O^i 2p orbitals to interact with the appropriate 4d wavefunctions of both bridged niobium atoms at the same time. Therefore, the resulting Nb−O^i−Nb π antibonding interactions can be significant and must be pointed out.

The results of our construction can be summarized as follows. The $2b_{1u}$ and $2b_{2g}$ dimer orbitals have bonding properties similar to that of the a_{2u} orbital, which is unoccupied in the monomeric cluster. Therefore, we expect the two orbitals of the dimer to be unoccupied as well. The $1a_{1g}$, $2a_{2u}$, $1e_g$, $1b_{1u}$, $1b_{2g}$, and $2e_g$ dimer orbitals all retain their dominant Nb 4d components responsible for Nb−Nb bonding. The $1a_{2u}$ and $1e_u$ orbitals loose the Nb 4d contributions at the shared vertex, but gain some of the lost Nb−Nb bonding back due to Nb 5p mixing. The intercluster Nb−O^i−Nb π antibonding in the $2a_{1g}$ orbital is balanced by the Nb−Nb bonding to the d_{z^2} orbital at the shared niobium atom. Thus, we expect all of these 12 orbitals to be occupied in the dimer, much like their parent orbitals are occupied in the monomeric cluster. The $2e_u$ orbital set, however, features not only substantial Nb−O^i−Nb π antibonding, but also a complete loss of bonding to the central niobium atom. If the destabilization of this level is strong enough, it may become unoccupied in the dimer.

This is exactly what happens. The computed correlation diagram between the molecular orbitals of the monomeric cluster and those of the dimer (using a Nb_6O_{17} fragment, "prepared" for condensation by removing one of the six O^a ligands, as an intermediate step) is shown in Figure 7. The $2e_u$ orbitals, now

(27) It can be shown, using the perturbation theory, for example, that the orbital destabilization due to a three-center Nb−O−Nb π antibonding interaction is about twice that due to a two-center Nb−O interaction, in accord with our intuition.

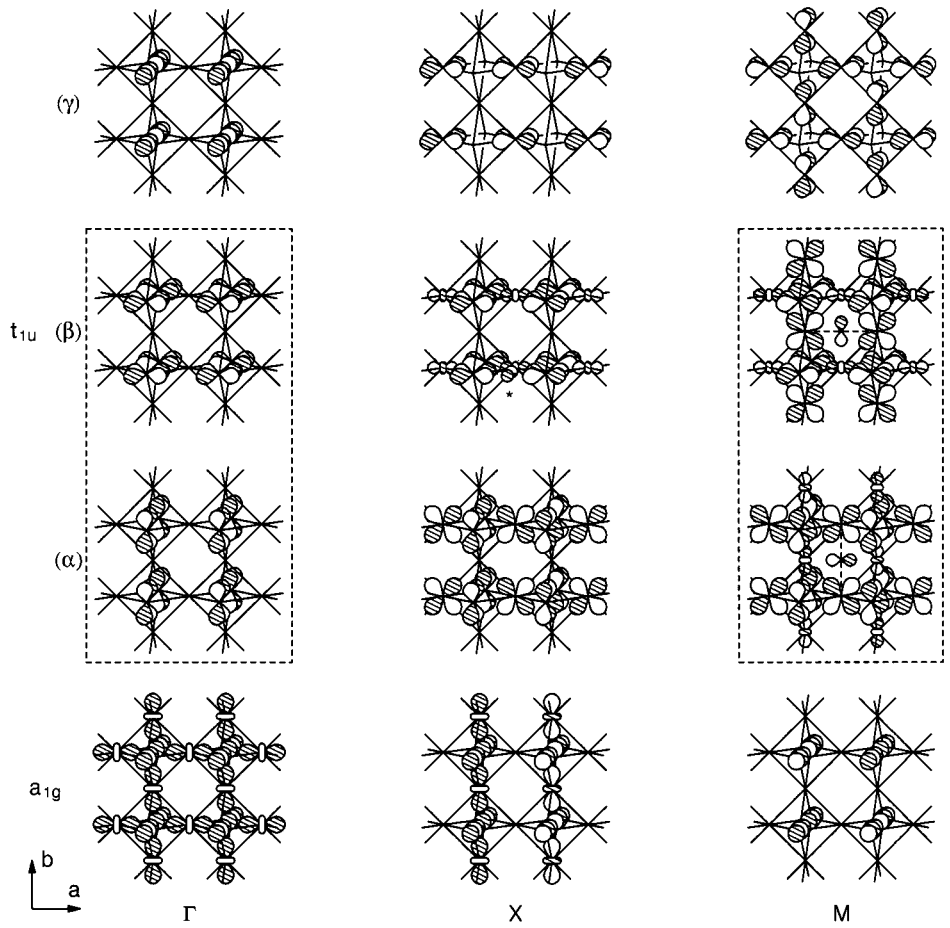

Figure 11. The a_{1g} and t_{1u} crystal orbitals of the square cluster network at $\Gamma = (0,0)$, $X = (\pi/a,0)$, and $M = (\pi/a,\pi/a)$. Degenerate orbitals are boxed together. A hard to notice oxygen 2p contribution to t_{1u} (β) at X is marked with an asterisk.

lying almost as high as the a_{2u}-like $2b_{1u}$ and $2b_{2g}$, are indeed pushed up in energy relative to the parent t_{2g} states. Twenty-four cluster electrons reside in the remaining MOs of the dimer, according to what is observed experimentally and consistent with the previous calculations.[6] Thus the "per octahedron" count is reduced from 14 electrons in Nb_6O_{18} to only 12.

We note that the actual molecular orbitals of the dimer, according to our calculations, do not look exactly like the ones constructed in Figure 6. As the point group is lowered from O_h (Nb_6O_{18}) to D_{4h} ($Nb_{11}O_{30}$), the molecular orbitals loose some of their symmetry; more orbital mixing takes place. For example, while the a_{1g} and t_{1u} orbitals are mutually orthogonal in the monomeric cluster, their derivatives in the dimer ($1a_{1g}$ and $2a_{1g}$, $1a_{2u}$ and $2a_{2u}$) may mix. As a result, the three inequivalent niobium atom sites have different contributions to the $1a_{1g}$ orbital, with the shared vertex contributing the most. Similar deviations from the icon-like shapes, sometimes significant, are observed in other molecular orbitals of the dimer as well. However, the overall shapes and bonding properties of all dimer orbitals can still be related to those of the parent a_{1g}, t_{1u}, t_{2g}, and a_{2u} icons.

A One-Dimensional Linear Chain of Clusters

The condensed cluster networks, which we consider next, are all infinite in their extent: a one-dimensional linear chain ([1 × 1 × ∞], Figure 2c), a two-dimensional square sheet ([1 × ∞ × ∞], Figure 2d), and the three-dimensional cubic network of NbO ([∞ × ∞ × ∞], Figure 2e). Zero-dimensional molecular orbitals evolve into crystal orbitals. Bands, with energies dependent on the position in a Brillouin zone, must be considered.[28,29]

In order to calculate a property of interest for an infinite periodic system, a numerical integration over a unique part of the Brillouin zone (irreducible wedge) has to be carried out. Typically tens or hundreds of sampling points (*k*-points) are needed to achieve reasonable accuracy.

It is possible to avoid, however, having to carry out our analysis at every *k*-point of such a large set.[30] We choose to examine crystal orbitals of condensed cluster networks only at high-symmetry (special) points of Brillouin zones, where both the orbital construction and bonding analysis are relatively easy to do.

The Brillouin zone for one-dimensional systems extends from $k = -\pi/a$ to $k = \pi/a$ with a half of the zone, from 0 to π/a, for example, sufficient to describe properties of the system under study (a is the lattice constant). Special *k*-points here are the Γ point at $k = 0$, with crystal orbitals not changing sign between neighboring unit cells, and X at $k = \pi/a$, with a phase change between neighboring cells. We will also use the $k = \pi/2a$ point, with a phase change taking place every two unit cells, for reasons which will become clear in a moment.

(28) Hoffmann, R. *Solids and Surfaces: A Chemist's View of Bonding in Extended Structures;* VCH: New York, 1988.
(29) Burdett, J. K. *Chemical Bonding in Solids;* Oxford University Press: New York, 1995.
(30) Our approach is related to the "fragment within a solid" method described in Burdett, J. K. *J. Am. Chem. Soc.* **1980**, *102*, 5458−5462 and the reciprocal space approach to the orbitals of truncated crystals developed in Wheeler, R. A.; Piela, L.; Hoffmann, R. *J. Am. Chem. Soc.* **1988**, *110*, 7302−7315.

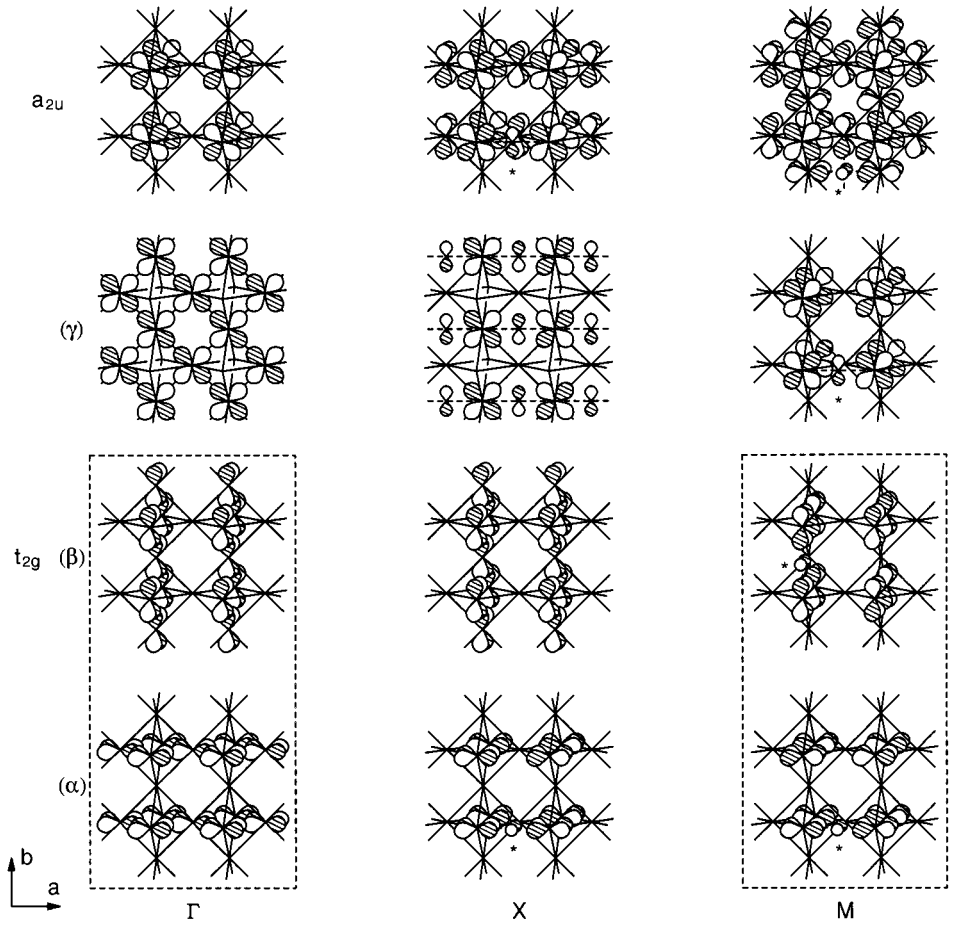

Figure 12. The t_{2g} and a_{2u} crystal orbitals of the square cluster network at $\Gamma = (0,0)$, $X = (\pi/a,0)$, and $M = (\pi/a,\pi/a)$. Degenerate orbitals are boxed together. Some hard to notice oxygen 2p contributions are marked with asterisks.

First, the orbital counting scheme is applied to the one-dimensional chain at Γ and X. The result is shown in Figure 8. The crystal orbitals of the chain look very similar to the molecular orbitals of the dimeric cluster (Figure 6). The a_{1g} band,[31] for instance, resembles the $1a_{1g}$ dimer orbital at the Γ point and the $1a_{2u}$ orbital at X, the t_{1u} (β) band is similar to the $2a_{2u}$ orbital at Γ and to the $2a_{1g}$ orbital at X, while the t_{1u} (α,γ) band looks much like $1e_u$ at Γ and $1e_g$ at X. The $1b_{1u}$ and $1b_{2g}$ dimer orbitals mimic the t_{2g} (β) band at Γ and X, respectively; in the same way the $2e_g$ and $2e_u$ orbitals approximate the t_{2g} (α,γ) band. The last of the considered bands, a_{2u}, resembles $2b_{1u}$ at Γ and $2b_{2g}$ at X.

Then, according to our previous analysis of the dimer, the a_{1g} band, all three t_{1u} bands, and the t_{2g} (β) band should be fully occupied in the chain, while the a_{2u} band should remain completely unoccupied. The t_{2g} (α,γ) band is expected to be filled at Γ, but empty at X, where both the Nb−O^i−Nb π antibonding between neighboring octahedra and the loss of Nb−Nb bonding are even more pronounced than in the $2e_u$ orbital of the dimer.

Thus we expect seven bands to be filled with 14 electrons at Γ and five bands to be filled with 10 electrons at X. One can naively estimate the optimized electron count to be $(10 + 14)/2 = 12$ per $Nb_4Nb_{2/2}$ by simply averaging over the two *k*-points which happen to have equal weights in the Brillouin zone.

(31) When refering to the bands and crystal orbitals of the $[1 \times 1 \times \infty]$, $[1 \times \infty \times \infty]$, and $[\infty \times \infty \times \infty]$ networks, we will use the a_{1g}, t_{1u}, t_{2g}, and a_{2u} labels in order to stress the relationship to the molecular orbitals of the monomeric cluster. The actual point group symmetry of the crystal orbitals, however, is often lower than O_h.

However, we really know only that the electron count maximizing bonding in the chain of clusters is between 10 and 14 electrons. Considering the crystal orbitals at the $k = \pi/2a$ point allows us to narrow down the window for the magic count. Figure 9 sketches one possible orbital representation of the partially filled t_{2g} (α,γ) band at this *k*-point. Comparing this drawing to the $2e_u$ dimer molecular orbital set in Figure 6, one finds that these orbitals have the same number of Nb−Nb bonding (four per two octahedra) and Nb−O^i−Nb antibonding (two per two octahedra) interactions. Thus the t_{2g} (α,γ) band should also be unoccupied at $k = \pi/2a$. The five bands filled at both Γ and X should remain filled at the $k = \pi/2a$ point because bonding properties of these bands change gradually across the Brillouin zone. Accordingly, the a_{2u} band should remain unoccupied at this *k*-point. There are two equivalent $k = \pi/2a$ points in the Brillouin zone ($k = \pm\pi/2a$), while Γ and X occur only once each. Therefore, the weighted averaging now yields $(14 \times 1 + 10 \times 2 + 10 \times 1)/4 = 11$ electrons per $Nb_4Nb_{2/2}$ octahedron. This is almost exactly the electron count observed in $Ba_{1-x}Nb_5O_8$.

Our calculations are also consistent with this result. The band structure for the one-dimensional linear chain of condensed niobium clusters is shown in Figure 10. An avoided crossing between the the t_{1u} (α,γ) and t_{2g} (α,γ) bands complicates the picture somewhat: the band right below the empty a_{2u} band is mainly t_{1u} (α,γ) around Γ and mainly t_{2g} (α,γ) around X. The optimal number of electrons is indeed 11: the occupied bottom of the partially filled band is weakly Nb−Nb bonding (because of a d_{z^2} mixing into t_{1u} (α,γ) similar to that shown in Figure

5a); the middle of this band has strong t_{2g} (α,γ) character (with the t_{1u} (α,γ) states providing further destabilization through mixing) and therefore is overall antibonding. This avoided crossing, as well as avoided crossings in band structure diagrams presented in the following sections, has little effect on the resulting magic counts.

A Two-Dimensional Square Network of Clusters

When four of the six vertices of a niobium octahedral cluster are shared, a two-dimensional square network is formed (Figure 2d). We proceed to analyze the crystal orbitals of this sheet using the approach just applied to the one-dimensional chain.

The corresponding two-dimensional Brillouin zone has three special points: Γ at $k = (0,0)$ with weight one, X at $(\pi/a,0)$ with weight two, and M at $k = (\pi/a,\pi/a)$ with weight one. The crystal orbitals at these k-points are constructed using the a_{1g}, t_{1u}, t_{2g}, and a_{2u} icons as shown in Figures 11 and 12.

Here we point out the increasing influence of the symmetry requirements imposed on crystal orbitals at a given k-point. For example, the band derived from the a_{1g} icon loses the Nb d_{z^2} contributions from four of six cluster atoms at M due to the requirement of a phase change along both lattice vectors at this k-point. Small Nb p_z contributions compensate for some of the lost Nb−Nb bonding.

None of the t_{1u}-based bands is substantially destabilized in energy due to the Nb−O^i−Nb π antibonding, but one of them, namely the t_{1u} (γ) band at Γ, simply loses all Nb $d_{xz,yz}$ contributions. As a result, only an out-of-phase combination of d_{z^2} orbitals on the unshared niobium atoms contributes to this crystal orbital. The Nb $p_{x,y}$ wavefunctions at the shared vertices could participate in bonding, but they are destabilized due to the interactions with the shared O^i ligands and do not contribute. Thus the t_{1u} (γ) band at Γ is expected to remain unoccupied as it lacks Nb−Nb bonding to counter Nb−O antibonding.

Cluster condensation in the $[1 \times \infty \times \infty]$ network has an effect on the t_{2g} bands similar to that in the chain and in the dimer: the Nb−O^i−Nb π antibonding interactions between neighboring octahedra and the loss of Nb−Nb bonding at the shared cluster vertices destabilize the α and γ components at X and all three components at M. All three t_{2g}-based crystal orbitals at the Γ point, as well as t_{2g} (β) at X, are essentially identical to their t_{2g} parent icons and thus are expected to be filled and to contribute to cluster bonding.

The a_{2u} band is another example of how the bonding character of a crystal orbital can depend on the symmetry at a particular k-point. While the Nb−O π antibonding, much like that in the parent a_{2u} orbital, dominates at the X and M points, the crystal orbital at Γ is made up only of the d_{xy} components of the unshared vertices. None of the oxygen orbitals, neither from the O^i nor from the O^a ligands, are allowed to mix in. The only interactions remaining are the long-range Nb−Nb π and δ-type ones, making this crystal orbital essentially nonbonding. One should expect then that it may be occupied in some compounds but may remain empty in others.

Therefore, the Γ point contributes 12 or 14 electrons, depending on whether the a_{2u} band is occupied or not, the X point contributes ten, and M contributes only eight. Bonding in such two-dimensional sheet of vertex sharing clusters should then be maximized at approximately $(12 \times 1 + 10 \times 2 + 8 \times 1)/4 = 10$ or $(14 \times 1 + 10 \times 2 + 8 \times 1)/4 = 10^1/_2$ electrons per $Nb_2Nb_{4/2}$ octahedron. Among the reported compounds containing the $[1 \times \infty \times \infty]$ cluster sheets KNb_4O_8 and $K_2Nb_5O_9$ have 9 electrons per cluster, $BaNb_4O_8$ has 10, and MNb_5O_9 (M = Ba, Sr, Eu) have 11 electrons per cluster. Such a spread may be in part attributed to the nonbonding nature of the a_{2u} band at Γ.

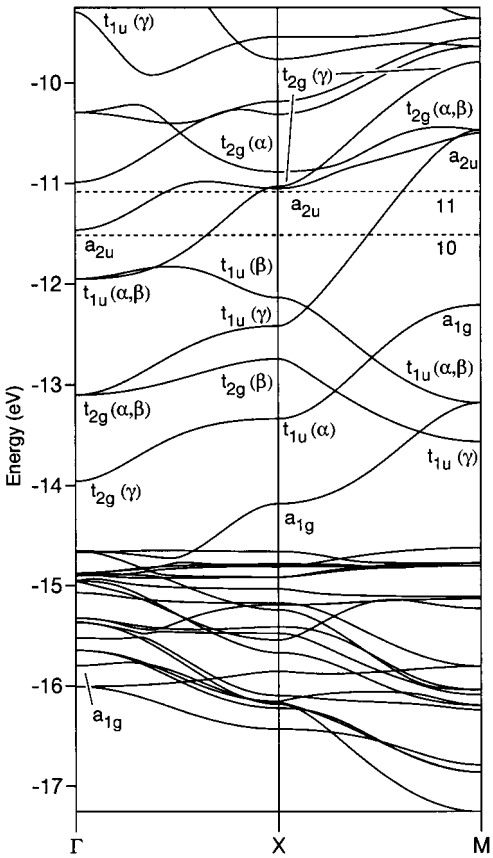

Figure 13. Computed band structure of the square cluster network. The unlabeled bands below −14.5 eV are oxygen 2p in character. Horizontal dashed lines indicate the positions of the Fermi level for 10 and 11 electrons per Nb octahedron.

The computed band structure (Figure 13) confirms our conclusions about which bands become destabilized and thus unoccupied. There are many avoided crossings taking place, but we do not discuss them as they are not crucial to our analysis. The Fermi levels plotted for 10 and 11 electrons per Nb_4 indicate that filling of the a_{2u} band at Γ is indeed the difference between these two counts. Another feature worth noting is that the bottom of the a_{1g} band (at Γ) dips into the oxygen 2p band. This is mainly the consequence of the fact that four of the six O^a ligands, which provided for σ antibonding with Nb d_{z^2}, are now missing.

NbO

When all vertices of the Nb_6O_{18} cluster participate in condensation, cubic NbO is formed. Its electronic structure has been studied previously at various levels of theory;[23,25] the analogy between bonding in NbO and Nb_6O_{18} has already been addressed.[4]

As before, we use the molecular orbitals of the monomeric cluster octahedron to construct the crystal orbitals of NbO at the following special points of the cubic Brillouin zone: Γ, with no phase change between opposite vertices of the niobium core, X, with a change of phase only along the a axis, M, with a change of phase along a and b, and R, with a sign change along all three axes. Figure 14 provides sketches of the crystal orbitals derived from the a_{1g}, t_{1u}, t_{2g}, and a_{2u} icons.

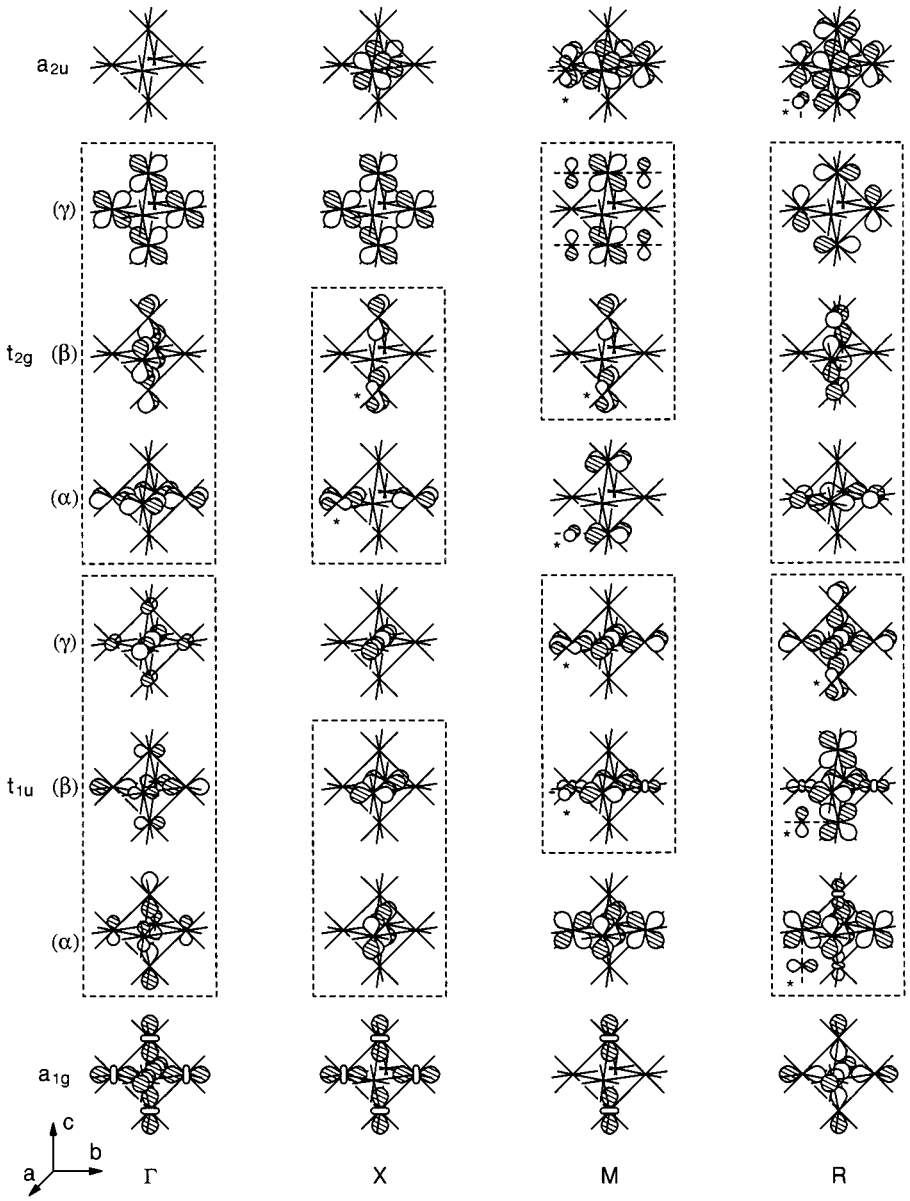

Figure 14. The a_{2g}, t_{1u}, t_{2g}, and a_{2u} crystal orbitals of the cubic NbO network at the Γ = (0,0,0), X = (π/a,0,0), M = (π/a,π/a,0), and R = (π/a,π/a,π/a) special points. Degenerate orbitals are boxed together. Some hard to notice oxygen 2p contributions are marked with asterisks.

The effects of the *k*-point symmetry requirements are evident as one traces any given crystal orbital from Γ to R. The a_{1g} band retains the d_{z^2} character at X and M, much like it happens in the linear chain and the square sheet of clusters, with the Nb p_z wavefunctions contributing to Nb−Nb bonding where d_{z^2} is not allowed to mix in. At the R point, however, the Nb d_{z^2} participation is not allowed at all; the corresponding crystal orbital is purely p_z in character. Despite the presense of Nb−Nb bonding, this orbital should lie somewhat high in energy due to the relatively high energy of the pure Nb 5p states (−6.86 eV).

The t_{1u} crystal orbitals, on the other hand, resemble their parent molecular orbitals of the monomeric cluster at R, with all Nb−Nb bonding retained. Perturbations introduced at M destabilize the t_{1u} (β,γ) components somewhat, but these are also expected to remain occupied, much like the t_{1u} (β) crystal orbital at X in the square sheet of clusters. The t_{1u} (α,β) crystal orbitals at X are also expected to remain filled, similar to the t_{1u} (α,β) orbitals of the square sheet at Γ. Continuing the analogy with the two-dimensional network, we notice that the t_{1u} (γ) crystal orbital of NbO at X resembles the t_{1u} (γ) of the square sheet at Γ. The latter was found to be unoccupied, we expect the same for its NbO analogue. No Nb 4d contribution is allowed at the Γ point; the mostly Nb 5p crystal orbitals should therefore remain unfilled, much like the a_{2g} band at R.

The behavior of the t_{2g} bands is somewhat similar to that of the a_{1g} band: at Γ all three of them look just like the t_{2g} orbitals of the monomeric cluster, but only the $p_{x,y}$ contributions remain at the R point, destabilizing these bands. The t_{2g} (α,β) components are destabilized at X in a way similar to the t_{2g} (α) band at the X point in the square sheet. All three bands are also expected to be unoccupied at M, where the t_{2g} (β,γ) components are comparable to the t_{2g} (α,β) set at M in the square sheet of clusters, and the t_{2g} (α) component is similar to t_{2g} (γ) at M of the same square sheet.

The a_{2u} band retains dominant Nb−O antibonding at R and M. However, it becomes essentially nonbonding at X, where it is made up only of the d_{xy} wavefunctions, analogous to the a_{2u} band of the square sheet at Γ. Neither any of the niobium nor

any of the oxygen wavefunctions are allowed to form a crystal orbital of local a_{2u} symmetry at the Γ point.

Careful readers may have noticed something of a trend in the evolution of the NbO crystal orbitals between the Γ and R points: there is a gradual change of balance between the Nb 4d and 5p contributions. This is no accident. A short paper-and-pencil exercise indeed confirms that the crystal orbitals with the *g* label (symmetric with respect to the inversion at the center of the niobium octahedron) at Γ and *u* label (antisymmetric with respect to the same symmetry operation) at R may have only Nb d and s contributions, while the *u*-labeled orbitals at Γ and the *g*-labeled ones at R may consist only of Nb p wavefunctions. Similar behavior of crystal orbitals was observed in a study of networks built from vertex-sharing aluminum octahedral clusters,[32] where only s and p wavefunctions of the metal site participated in bonding.

Noting that the relative weights of the Γ, X, M, and R special points in the cubic Brillouin zone are one, three, three, and one, respectively, we proceed with our orbital counting scheme. The Γ point is expected to contribute the a_{1g} and all three t_{2g} bands to the magic electron count; the X point contributes a_{1g}, t_{1u} (α,β), t_{2g} (γ), and perhaps the nonbonding a_{2u}; the a_{1g} and all three t_{1u} bands should be filled at the M point; the R point contributes only the t_{1u} bands. Averaging over the Brillouin zone yields $(8 \times 1 + 8 \times 3 + 8 \times 3 + 6 \times 1)/8 = 7^3/_4$ or $(8 \times 1 + 10 \times 3 + 8 \times 3 + 6 \times 1)/8 = 8^1/_2$ electrons per $Nb_{6/2}$ octahedron, depending on whether the a_{2u} band at X is occupied. NbO itself has nine electrons per octahedron which are responsible for Nb−Nb bonding.

The computed band structure for NbO is plotted in Figure 15; it confirms our qualitative orbital counting scheme. The cluster count of eight electrons corresponds to four Nb−Nb bonding bands filled at Γ, X, and M, and three filled bands at R. As the number of electrons per octahedron increases, the essentially nonbonding a_{2u} band at X is filled. At nine electrons per octahedron the t_{2g} (α,β) states at X also become occupied.

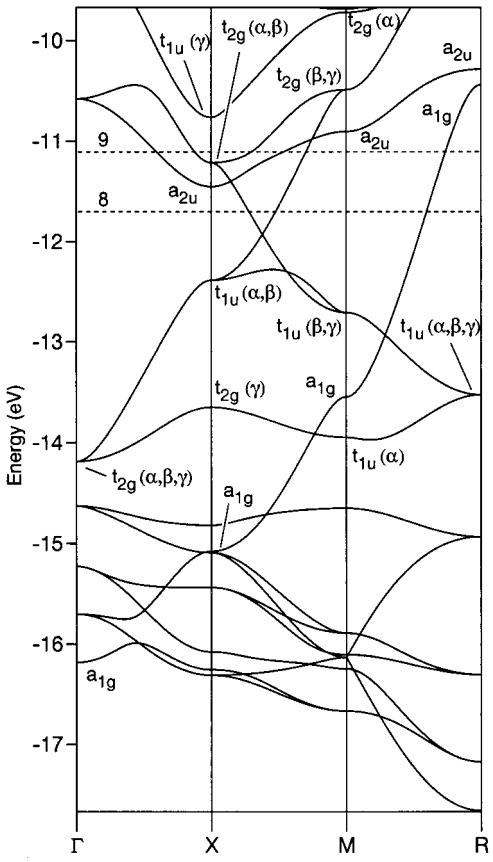

Figure 15. Computed band structure of NbO. The unlabeled bands below −14.5 eV are oxygen 2p in character. Horizontal dashed lines indicate the positions of the Fermi level for 8 and 9 electrons per Nb octahedron.

Table 2. Expected Magic Electron Counts (per Nb octahedron) for Some Networks of Condensed Oxoniobate Clusters Compared to the Observed Cluster Electron Counts and to the Results of the Previously Reported Counting Scheme[a]

network	predicted[b] (this study)	observed[3]	predicted[3]	Nb atoms per octahedron
$[1 \times 1 \times 1]$	14	13−15	14^c	6
$[1 \times 1 \times 2]$	12	$11^1/_2$−12	$11^5/_6{}^c$	$5^1/_2$
$[1 \times 1 \times \infty]$	11	11	11	5
$[1 \times \infty \times \infty]$	10−$10^1/_2$	9−11	10	4
$[\infty \times \infty \times \infty]$	$7^3/_4$−$8^1/_2$	9	9^c	3

[a] According to this counting scheme, shared niobium atoms contribute three electrons each to cluster bonding, neighboring unshared niobium atoms add two electrons each to the count, and all other unshared vertices contribute $2^1/_3$ electrons each.[3] [b] Assuming that the Nb−O π antibonding in the a_{2u} molecular orbital and its derivatives outweighs the Nb−Nb bonding interactions. [c] Used as reference points in constructing the counting scheme.

Conclusions

We have shown in detail how the molecular orbitals of the dimeric $Nb_{11}O_{30}$ cluster and the crystal orbitals of the $[1 \times 1 \times \infty]$, $[1 \times \infty \times \infty]$, and $[\infty \times \infty \times \infty]$ networks of oxoniobate clusters with octahedral Nb_6 core condensed through vertex-sharing can be related to the molecular orbitals of the monomeric Nb_6O_{18} cluster itself. Moreover, by carefully considering the effects of vertex-sharing on the bonding properties of these states we were able to derive approximate cluster electron counts for the above-mentioned networks, which closely match the experimentally observed counts and agree with our electronic structure calculations.

The orbital counting scheme developed in this study can be summarized in the following way. First, the electronic structure of the monomeric cluster and the dimer were examined. This analysis, as earlier ones,[3,6] highlighted the Nb−O−Nb π antibonding across the linear bridges and the loss of Nb−Nb bonding at the shared vertex, which were responsible for the destabilization of the $2e_u$ orbital set in the dimer. Depopulation of the $2e_u$ set, derived from the t_{2g} molecular orbitals of the monomeric cluster, lead to a reduction of the "per octahedron" electron count from 14 in the monomeric cluster to 12 in the dimer. Thus all t_{2g} -based crystal orbitals of the three extended networks with similar features were expected to be unoccupied as well. In addition, symmetry restrictions imposed on crystal orbitals at a given *k*-point in reciprocal space proved to be powerful in eliminating in some cases important niobium contributions responsible for the Nb−Nb bonding.

In the end, weighted averaging over the considered special points yielded magic cluster electron counts for the extended networks. These are summarized in Table 2, along with the experimentally observed counts and the results of the previously reported counting scheme.

Not only the optimal cluster electron count changes as vertex-sharing takes place. The number of niobium atoms per Nb octahedron changes as well. So, there are six niobium atoms in the monomeric Nb_6O_{18} unit, five and a half in the dimer, five

(32) Vajenine, G. V.; Hoffmann, R. *J. Am. Chem. Soc.* **1998**, *120*, 4200−4208.

in the linear chain, four in the square sheet of clusters, and only three in NbO. A comparison of the NbO and TiO structures is helpful (the latter is built from linear cluster chains, as in Figure 2c). Since the metal atoms in both compounds are formally divalent, each niobium atom contributes three electrons and each Ti atom contributes two electrons to metal−metal bonding. Let us consider four possibilities: (a) NbO itself, (b) TiO with the NbO structure, (c) NbO with the TiO structure, and (d) TiO itself.

The first possibility corresponds to a network with three metal atoms per octahedron, each contributing three electrons, or a total of nine. The second case brings us only up to six electrons for the same network. In (c), five atoms per octahedron contribute the total of 15 electrons, while the electron count in (d) is only ten. Table 2 suggests that six electrons per octahedron are too few for the [$\infty \times \infty \times \infty$] network, while 15 electrons are too many for the [$1 \times 1 \times \infty$] network. The cases (a) and (d) match well the expected cluster counts of Table 2; they correspond to actual compounds.

We expect analogous direct relationships between molecular orbitals of other monomeric metal clusters and molecular or crystal orbitals of their condensates. Such analysis will complement the existing knowledge of chemical bonding in condensed cluster networks.[33] In particular, other modes of octahedral cluster condensation, edge-sharing,[34] and face-sharing,[35] can be addressed. Condensation of clusters with interstitials should also be considered.

Acknowledgment. Thanks are due to the Max-Planck Society and the Alexander von Humboldt Foundation for providing Grigori Vajenine with financial support during this study. We also thank Dr. Jürgen Köhler for helpful discussions.

IC981460K

(33) See ref 2 and references therein.

(34) Oxomolybdates containing trans-edge-sharing $Mo_6O^i_{12}$ octahedra are perhaps the best example of this condensation mode. For discussion of bonding, see Hughbanks, T.; Hoffmann, R. *J. Am. Chem. Soc.* **1983**, *105*, 3528−3537 and Wheeler, R. A.; Hoffmann, R. *J. Am. Chem. Soc.* **1988**, *110*, 7315−7325. We note that edge-sharing in this case, unlike the vertex-sharing in oxoniobates, removes some of the inner-sphere ligands.

(35) Linear one-dimentional chains of face-sharing $M_6X^i_8$ clusters are found in some ternary molybdenum and iron chalcogenides. The bonding in these systems is discussed in Nohl, H.; Klose, W.; Andersen, O. K. In *Superconductivity in Ternary Compounds I;* Fischer, Ø., Maple, M. B., Eds.; Springer: New York, 1982; pp 165−221. Kelly, P. J.; Andersen, O. K. In *Superconductivity in d- and f-Band Metals;* Buckel, W., Weber, W., Eds.; Kernforschungszentrum Karlsruhe, 1982; pp 137−140. Hughbanks, T.; Hoffmann, R. *Inorg. Chem.* **1982**, *21*, 3578−3580. Hughbanks, T.; Hoffmann, R. *J. Am. Chem. Soc.* **1983**, *105*, 1150−1162. Face-sharing between $M_6X^i_8$ clusters also leads to a loss of some of the inner-sphere ligands.